

# Diagenetic processes and sediment–water exchanges of heavy metals in the Mejerda River Delta (Gulf of Tunis)

Mohamed Amine Hellali<sup>1</sup> · Nouredine Zaaboub<sup>2</sup> · Walid Oueslati<sup>1</sup> · Ayed Added<sup>1</sup> · Lotfi Aleya<sup>3</sup>

Received: 24 December 2014 / Accepted: 15 June 2015 / Published online: 29 June 2015  
© Springer-Verlag Berlin Heidelberg 2015

**Abstract** An in situ benthic flux study of iron (Fe), manganese (Mn), lead (Pb), zinc (Zn), cadmium (Cd), copper (Cu) and cobalt (Co) was conducted at three stations at the Mejerda River outlet in the Gulf of Tunis, at depths of 10, 20 and 40 m in March and August 2012. Simultaneously, three sedimentary cores were taken at the same locations to evaluate the diffusive flux of these heavy metals and to determine the early diagenetic mechanisms occurring below the sediment–water interface and their impact on heavy metal mobility. The concentrations of  $\text{Fe}^{2+}$  in pore waters were similar to those observed in the rest of the Gulf of Tunis; flux, both benthic ( $275 \mu\text{mol m}^{-2} \text{day}^{-1}$ ) and diffusive ( $9 \mu\text{mol m}^{-2} \text{day}^{-1}$ ), confirmed that sediment was a source of  $\text{Fe}^{2+}$  for the water column, at least for the 10- and 20-m stations. The diffusive flux of  $\text{Mn}^{2+}$  was greater in August ( $11\text{--}14 \mu\text{mol m}^{-2} \text{day}^{-1}$ ) than in March ( $1\text{--}2.6 \mu\text{mol m}^{-2} \text{day}^{-1}$ ), representing 8–15 % of benthic flux and indicating that, as for Fe, sediment is a source of  $\text{Mn}^{2+}$  for the water column, especially in August.  $\text{Mn}^{2+}$  is produced before  $\text{Fe}^{2+}$ , which corresponds to the overall pattern of early diagenesis. In March, the production of  $\text{Mn}^{2+}$  and  $\text{Fe}^{2+}$  takes place in the lower layers of the sediment, probably due to agitation and resuspension occurring at the sediment–water interface. The concentrations of  $\text{Pb}^{2+}$  and

$\text{Zn}^{2+}$  were higher in this study with reference to the corresponding concentrations in the coastal areas, revealing an anthropogenic activity on the Mejerda River, Ghar El Melh Lagoon (old Mejerda outlet) and the Khlij Channel as the main vectors.

**Keywords** Late diagenesis · Benthic flux · Diffusive flux · Sediment–water exchanges · Heavy metals · Tunisia

## Introduction

In recent decades, degradation of coastal ecosystems has become a serious problem worldwide. Due to human activities generating excess organic matter and heavy metals, the organisms inhabiting these environments must tolerate high levels of polluting loads (Belabed et al. 2013; Zaaboub et al. 2014a). In Tunisia, one of the regions most affected by anthropogenic pressure is the Gulf of Tunis located in the northeastern part of the country and whose coastal area has deteriorated due not only to its sediment budget and shoreline retreat (Brahim et al. 2015), but also to heavy metals discharged into the gulf via the Mejerda River and the neighboring river systems of the Ghar El Melh Lagoon, the Ariana Sabkha (*sabkha* in Arabic designates a coastal and inland saline mud flat built up in shallow depressions through deposition of silt, clay and sand) and the Khlij Channel (Essoni 1998; Zaaboub et al. 2014b). In the gulf's deeper sediments fine grain size distribution is dominant, clay and fine silt particles being predominant at depths >25 m (75–95 %). Concerning mineralogy, quartz distribution indicates a homogenous size distribution over the Mejerda River Delta, with an average of 30 %. In the fine fraction the quartz average was around 8 %, with two distribution areas: one near Ghar El Melh Lagoon and the other in the lower

✉ Lotfi Aleya  
lotfi.aley@univ-fcomte.fr

<sup>1</sup> Laboratoire des Ressources Minérales et Environnement, Département de Géologie, Faculté des Sciences de Tunis, Université Tunis-El Manar, 2092 Tunis, Tunisia

<sup>2</sup> Laboratoire du Milieu Marin, Institut National des Sciences et Technologies de la Mer, 2025 Salammbô, Tunisia

<sup>3</sup> Laboratoire de Chrono-Environnement, UMR CNRS 6249, Université de Bourgogne Franche-Comté, La Bouloie, 25030 Besançon Cedex, France

Mejerda River (Zaaboub et al. 2014b). Heavy metals arriving in the gulf settle to the bottom where exchanges between sediment and water take place under the effect of physical, chemical and biological variables (Alaoui and Aleya 1995; Warnken et al. 2001). However, despite accumulation of heavy metals in the biomass, with long biological half-lives which can cause health hazards (Ben Salem et al. 2014), no information is available on the potential upward release of heavy metals at the sediment–water interface in the Mejerda Delta located in the western Gulf of Tunisia. Previous studies have dealt only with pore water geochemistry (Essoni 1998), sediment geochemistry (Essoni 1998; Helali 2010) and sediment dynamics along with currents (Brahim et al. 2015).

The aim of this study was thus to investigate, for the first time to our knowledge, the potential exchanges of heavy metals [iron (Fe), manganese (Mn), lead (Pb), zinc (Zn), cobalt (Co), copper (Cu) and cadmium (Cd)] at the sediment–water interface in the Mejerda Delta. Benthic chambers were deployed and core samples were taken at three stations during two different months, March and August 2012, corresponding to spring and summer (dry and wet seasons respectively).

## Materials and methods

### Study area

The Mejerda River Delta is located in the western Gulf of Tunisia. The Mejerda is the most important river in Tunisia and the main source of water and sediments brought to the gulf, with an approximate water flow rate of  $30 \text{ m}^3 \text{ s}^{-1}$  and sediment flow rate of  $10\text{--}30 \text{ g l}^{-1}$  (Essoni 1998). The outlet is, in fact, now an artificial channel constructed in 1973 to evacuate flood waters. The delta area is also influenced by the Khlij Channel, Ghar El Melh Lagoon and Ariana Sabkha, which may or may not be in direct contact with marine water (Fig. 1). The Mejerda River has also been the subject of several studies, particularly as regards the displacement of the river outlet over the last centuries (Mauldenhauer et al. 2008). Facing the mouth of the Mejerda, sediment grain size showed that clay and fine silt particles are dominant (75–95 %). For mineralogy, the clay fraction is dominant with more than 70 % (Zaaboub et al. 2014b).

This study was conducted at 3 stations in the Gulf of Tunisia at depths of 10 m ( $37^{\circ}0.468' \text{N } 10^{\circ}13.821' \text{E}$ ), 20 m ( $37^{\circ}0.440' \text{N } 10^{\circ}16.188' \text{E}$ ) and 40 m ( $37^{\circ}0.419' \text{N } 10^{\circ}17.881' \text{E}$ ), respectively, forming a perpendicular radial to the coast and offshore from the mouth of the Mejerda River (Fig. 1). Sites were selected off shore, facing the outlet and samples were taken in March and August 2012.

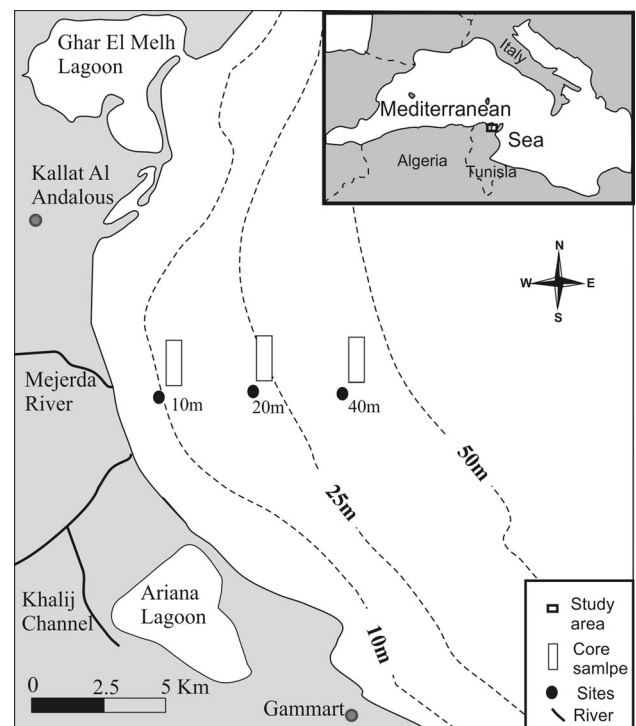


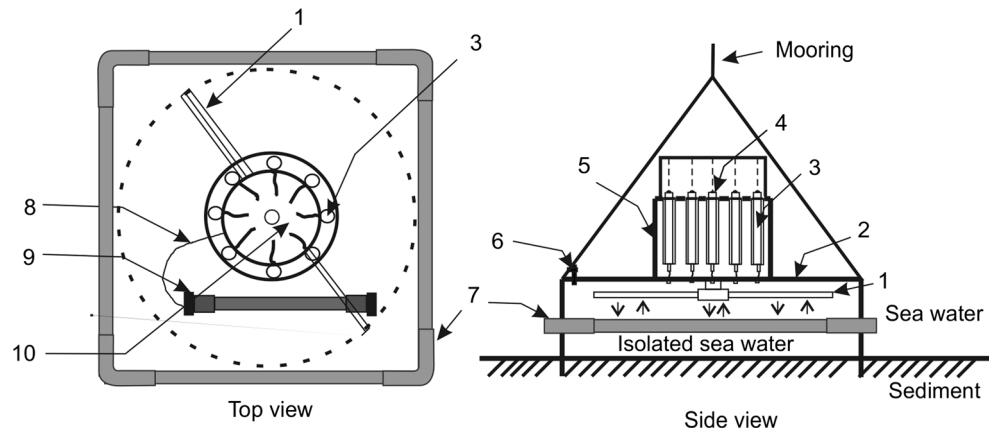
**Fig. 1** Study area and sampling locations

A benthic chamber was used for both water and core sediment samples.

### Sediment cores

For core sampling timing, cores were collected just after benthic chamber deployment so as not to disturb the sediment and thus avoid resuspension problems. Given that at depths of 10–40 m the sediment is composed of fine fraction and, as reported by Helali et al. (2013) and Zaaboub et al. (2014b), that it becomes muddy in these depths, this procedure ensured protection of the fine sediment quality in the cores. The cores were recovered using polyvinyl chloride pipes ( $\varnothing 50 \text{ mm}$  and length 50–90 cm). Under an inert atmosphere ( $\text{N}_2$ ) and using a Glover bag, the sediment was sliced into sections of 1–2 cm thick at the top of the cores (0–20 cm) and sections of 5 cm for the rest because the highest variations of dissolved heavy metals are observed in the first centimeters below the water–sediment interface. After measurement of pH and Eh (82862 Weilheim WTW), each section was placed in a polypropylene beaker previously washed with double distilled water (Milli-Q) and sealed within an inert atmosphere. The beaker was centrifuged at 3500 rpm for 20 min to separate pore water from sediment and then passed through a  $0.45 \mu\text{m}$  filter.

**Fig. 2** Benthic chamber diagrams. Transparent benthic chamber: 1 stirrer, 2 PVC bottom, 3 sampling syringe, 4 pressure control syringe, 5 motor chamber, 6 control valve, 7 ballast, 8 water proof electric cables, 9 battery, 10 flexible membrane



*Benthic chambers*

The benthic chambers were square-shaped boxes with a total capacity of 37.5 l and covered a sediment area of 0.25 m<sup>2</sup>. Made of transparent polymethylmethacrylate (PMMA) 6 mm thick, they also contained a stirrer made of PMMA, which rotated at a speed of 8 rpm. Before sampling, the chamber’s stirrer was switched on for 8 min (Fig. 2). To avoid contamination, all the chamber components were made of PMMA; no metal component was in contact with the incubated water. A total of nine 60 ml syringes were placed outside the chamber and connected to the interior by a 3-mm-diameter silicone pipe. The chambers were cleaned with double distilled water (Milli-Q) and ultrapure HNO<sub>3</sub> (5 %) before deployment on the sea floor at the sediment–water interface; care was taken so as not to disturb sediment particles. An electronic timer controlled the stepping motor mechanism that triggered the filling of each syringe every 2.5 h. The first sample of water ( $t = 0$ ) was collected a few centimeters above the sea floor, taken manually (or with syringes) by a diver. We left ~15 min between each chamber deployment at different depth sites. The total sampling time chosen for benthic chamber incubation experiments was 24 h since a longer period results in highly anoxic water. In such conditions, flux exchanges between sediment and water will be heavily modified and other phenomena will also be observed, as reported in Ghar El Melh Lagoon and the Gulf of Tunis (Added 2002).

*Trace metal analysis*

An iron co-precipitation technique (Welch et al. 1990) was used to concentrate the dissolved heavy metals in both pore and benthic water samples. To each 5 ml of water sample, 100 μl of 1 M FeNO<sub>3</sub> solution (pH 7) was added; the precipitate thus formed was recovered with a 0.45-μm filter and dissolved in 10 % HNO<sub>3</sub> solution. Concentrations of Mn<sup>2+</sup>, Pb<sup>2+</sup>, Zn<sup>2+</sup>, Cu<sup>2+</sup>, Cd<sup>2+</sup> and Co<sup>2+</sup> were determined with a Thermo Scientific GFAAS (FS95 SOLAAR). The

Fe<sup>2+</sup> concentration was determined directly from the raw sample with a Thermo Scientific ICE 3300 AA Spectrometer. A water sample was treated in ten replicates and analyzed for seven heavy metals to estimate precision [relative standard deviation (RSD)] (Added 2002).

*Theoretical calculations*

Diffusive flux ( $J$ ) of a dissolved component was calculated from the pore water profile according to Fick’s first law:  $J = -\Phi \cdot D_{\text{sed}} \cdot \left(\frac{dC}{dx}\right)$  where  $\frac{dC}{dx}$  represents the gradient at the sediment–water interface (Schulz and Zabel 2006). To use Fick’s first law, sediment was considered to be in steady state. The negative sign indicated that the flux was directed to the opposite side of the concentration gradient, meaning that when the concentration increased with depth below the sediment–water interface, the flux was directed to the water column.  $\Phi$  represents sediment porosity,  $D_{\text{sed}}$  represents the molecular diffusion coefficient in the sediment, while  $D_{\text{sed}} = D^{\text{sw}}/\theta^2$  and  $\theta^2 = 1 - \ln(\Phi^2)$  which is related to the tortuosity “ $\theta$ ”, temperature and chemical elements, according to Boudreau (1997).

Benthic flux was determined from a time versus concentration diagram. An average gradient  $\frac{dC}{dt}$  was then selected while trying to best represent the average measurement points. Subsequently, benthic flux ( $J_b$ ) was determined by the equation:  $J_b = \frac{dC}{dt} \times h$  (in mmol m<sup>-2</sup> day<sup>-1</sup>) where  $\frac{dC}{dt}$  is given in μM/h and  $h$  denotes the height of the benthic chamber in meters (Added 2002).

The thermodynamic software PHREEQC 3.0 was used to estimate the saturation index for principal mineral species (Oueslati 2011).

**Results**

- pH profiles showed the same evolution at the three stations in March and August. There was a sudden

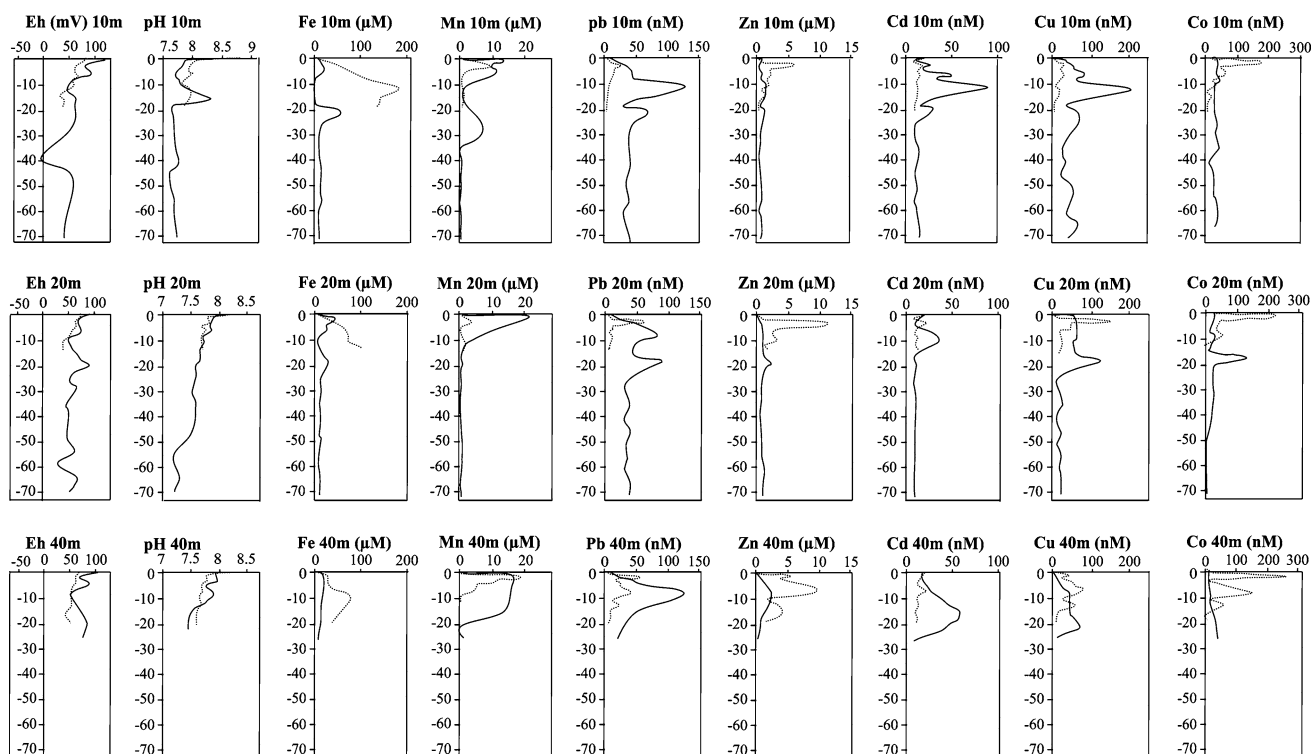


**Fig. 3** Pore water profiles of pH, Eh and heavy metals at the stations 10, 20 and 40 m (dash line March and continues line August)

decrease from the passage from the sediment–water interface (Fig. 3). The pH measured at the bottom of the water column was 8.15–8.3, depending on the season, dropping to <7.9 just below the sediment–water interface. However, it continued to decrease along the cores until it reached a value of 7.3–7.2 at >20 cm below the interface.

- **Eh** The redox values decreased rapidly from the sediment–water interface, from >400 mV in the water column, indicating an oxic environment to <100 mV from the first few centimeters of sediment with no seasonal variation. The decrease in redox potential at the lower core depth became progressive in the sediment, but the values remained positive even at 70-cm depth. This finding reflects slightly reduced conditions in sediment (Fig. 3).
- **Iron**

**Pore water** Concentrations of  $\text{Fe}^{2+}$  vary greatly between seasons (Table 1). In March, the concentration was >80  $\mu\text{M}$  at the 20- and 40-m stations and reached almost 200  $\mu\text{M}$  at the 10-m station. In August, the highest value did not exceed 50  $\mu\text{M}$  at any of the three stations. Most of the changes in the concentration of  $\text{Fe}^{2+}$  occurred in the first 10 cm of the sediment (Fig. 3). Since the concentrations of  $\text{Fe}^{2+}$  were very low in the water column (<3  $\mu\text{M}$ ), all

the profiles showed an enrichment of this element just below the sediment–water interface.

**Incubated water** The highest levels were observed in the waters of the benthic chambers in March, with the concentration varying from 4  $\mu\text{M}$  at the beginning of the study to 6  $\mu\text{M}$  after 24 h. In contrast, in August the concentration did not exceed 3  $\mu\text{M}$  even after 24 h (Fig. 4). At the 10- and 20-m stations, flux variations were slightly greater in March; in situ measurements showed benthic fluxes of 230, 384 and 220  $\mu\text{mol m}^{-2} \text{day}^{-1}$  at the 10-, 20- and 40-m stations, respectively, whereas they were 190  $\mu\text{mol m}^{-2} \text{day}^{-1}$  at the 10- and 20-m stations in August (Table 3). The 40-m station in particular showed a slight reverse flux ( $-38 \mu\text{mol m}^{-2} \text{day}^{-1}$ ), but analysis was conducted for only 15 h due to technical limitations.

- **Manganese**

**Pore water** Concentrations of  $\text{Mn}^{2+}$  did not exceed 22  $\mu\text{M}$  at the three stations. Manganese production begins at the sediment–water interface, thus explaining why the profiles showed a relatively strong gradient there. The  $\text{Mn}^{2+}$  peak occurred at different levels, depending on the season; a peak was noted  $\sim 3$  cm below the sediment–water

**Table 1** Heavy metal concentrations in pore water

	Depth (cm)	Fe (μM)	Mn (μM)	Pb (nM)	Zn (μM)	Cd (nM)	Cu (nM)	Co (nM)
Detection limits		0.11	0.0005	0.02	0.00011	0.17	0.55	0.8
RSD (%)		0.25	1.53	2.29	3.33	0.32	1.72	0.9
March (10 m)	1	2.27	0.35	6.00	0.25	20.99	2.40	14.21
	0	33.47	3.52	6.94	0.01	12.51	5.04	38.54
	−1	40.02	5.59	11.14	0.94	10.59	13.90	174.70
	−2	58.94	11.44	24.91	5.90	17.17	25.52	115.63
	−3	60.39	5.06	17.28	4.15	15.88	20.29	43.56
	−4	71.30	2.81	14.81	2.03	14.45	23.48	59.03
	−6	90.40	0.48	14.23	2.41	16.70	23.61	55.75
	−8	124.24	0.09	8.04	1.82	13.69	15.28	22.45
	−10	183.91	0.2	6.15	2.16	13.28	6.88	27.69
	−12	166.53	0.94	5.69	0.76	12.9	15.84	4.70
March (20 m)	1	2.07	0.18	6.60	0.22	23.24	1.20	13.21
	0	26.25	0.91	8.81	0.01	11.01	1.89	80.21
	−1	44.53	1.65	10.74	0.86	12.17	8.19	220.69
	−2	40.38	3.22	60.67	11.13	25.26	155.19	153.4
	−3	55.28	0.03	33.99	10.21	16.89	54.20	41.08
	−4	59.83	0.03	11.70	4.27	14.73	44.67	40.68
	−5	65.70	0.03	13.94	3.07	13.96	52.15	37.48
	−6	71.37	0.06	5.91	2.34	12.09	17.65	30.86
	−8	77.91	0.11	10.78	3.23	14.47	20.80	52.60
	−10	75.35	1.82	6.52	1.39	12.67	26.15	28.83
March (40 m)	1	2.89	0.18	3.00	0.12	19.46	1.28	14.81
	0	25.56	1.82	5.79	0.01	19.13	34.58	22.04
	−1	30.19	18.35	55.04	5.23	16.95	41.45	264.68
	−2	28.92	12.23	18.75	3.81	13.30	23.72	209.39
	−3	30.37	10.16	28.09	5.40	14.46	57.11	5.61
	−4	30.92	4.70	22.86	5.72	12.40	56.58	47.30
	−6	49.11	4.54	42.51	9.69	21.87	82.62	82.54
	−8	77.31	BDL	33.54	7.69	12.80	51.68	154.18
	−10	77.31	0.08	11.89	1.99	12.01	24.02	11.45
	−12	68.58	0.05	23.55	3.63	15.84	59.16	63.40
August (10 m)	1	62.92	0.01	7.69	3.86	10.90	16.43	38.77
	0	55.36	0.03	10.93	3.72	11.66	14.87	2.30
	−1	41.57	0.05	6.39	1.59	11.52	8.87	5.02
	−2	1.90	0.78	6.23	0.25	21.23	3.83	24.97
	−4	10.48	12.98	19.39	0.88	13.77	29.92	39.13
	−6	14.60	9.74	27.85	0.50	27.25	46.08	42.48
	−8	24.74	11.49	44.24	0.68	20.12	56.29	42.48
	−10	11.22	9.37	45.09	0.98	49.73	82.80	39.80
	−12	0.40	4.95	52.09	0.66	33.89	58.83	49.81
	−15	3.94	2.00	125.15	1.65	86.44	141.80	27.68
	0.28	1.20	118.34	1.55	85.96	208.97	29.03	
	2.48	1.53	66.35	1.34	34.93	106.00	31.73	

**Table 1** continued

	Depth (cm)	Fe ( $\mu\text{M}$ )	Mn ( $\mu\text{M}$ )	Pb (nM)	Zn ( $\mu\text{M}$ )	Cd (nM)	Cu (nM)	Co (nM)
	-18	7.47	3.13	28.83	0.62	15.04	32.29	33.08
	-20	58.00	4.26	69.01	1.36	29.53	58.79	30.01
	-25	17.21	6.33	45.83	0.89	11.01	66.58	40.47
	-30	14.66	6.32	40.24	0.53	11.26	38.15	32.41
	-35	8.78	BDL	39.90	0.56	12.94	21.68	43.81
	-40	15.70	0.74	39.19	0.61	14.82	29.95	14.75
	-45	14.35	0.10	38.19	0.69	10.35	20.84	27.00
	-50	12.90	0.03	34.62	0.87	13.14	48.58	29.03
	-55	14.86	0.14	38.61	0.76	11.26	44.14	32.41
	-60	12.87	0.12	29.42	0.58	12.87	33.44	41.81
	-65	12.6	0.39	32.72	1.07	15.35	64.49	31.73
	-70	10.87	0.34	36.97	0.75	15.63	38.53	31.65
August (20 m)	1	1.67	0.91	6.50	0.18	22.03	2.40	37.12
	0	17.33	21.48	17.63	0.51	13.77	44.66	24.97
	-2	41.03	17.46	31.33	0.64	11.95	58.88	26.32
	-4	30.16	12.90	57.28	0.98	13.23	61.55	20.89
	-6	27.44	7.90	77.02	1.13	31.03	63.81	22.25
	-8	17.92	5.33	85.32	1.10	35.50	63.54	13.38
	-10	7.31	1.84	56.45	1.11	35.98	56.23	32.41
	-15	17.97	0.42	45.31	1.02	10.75	61.51	14.07
	-18	28.35	0.56	89.65	2.16	11.65	125.9	130.26
	-20	25.53	0.25	68.35	1.20	11.38	72.83	29.71
	-25	13.53	BDL	39.88	0.90	10.49	11.03	21.13
	-30	15.92	0.22	32.05	0.80	10.55	15.89	22.25
	-35	13.13	0.30	39.23	0.73	10.64	23.81	23.13
	-40	14.64	0.39	30.58	0.59	10.47	5.17	18.85
	-45	12.60	0.44	40.83	0.70	10.32	17.32	13.07
	-50	14.37	0.45	34.09	0.71	10.66	9.95	0.39
	-55	10.56	0.60	38.28	0.87	11.02	18.38	0.45
	-60	12.15	0.68	32.02	1.10	10.00	15.74	0.35
	-65	12.64	0.35	41.55	0.94	10.00	18.65	0.24
	-70	12.70	0.55	39.93	0.91	10.00	21.04	0.24
August (40 m)	1	1.17	1.35	10.49	0.26	17.44	2.51	5.76
	0	19.98	16.42	25.88	0.30	17.27	4.03	11.61
	-2	22.84	16.35	38.08	0.81	16.2	11.44	7.59
	-4	22.13	15.54	77.27	1.40	23.4	20.1	11.61
	-8	19.48	14.94	127.08	2.58	32.94	45.22	15.24
	-15	16.22	12.97	49.44	1.25	57.32	47.38	24.59
	-20	13.57	0.28	32.05	0.58	44.08	74.01	36.86
	-25	10.45	0.92	19.84	0.31	10.00	10.141	44.02

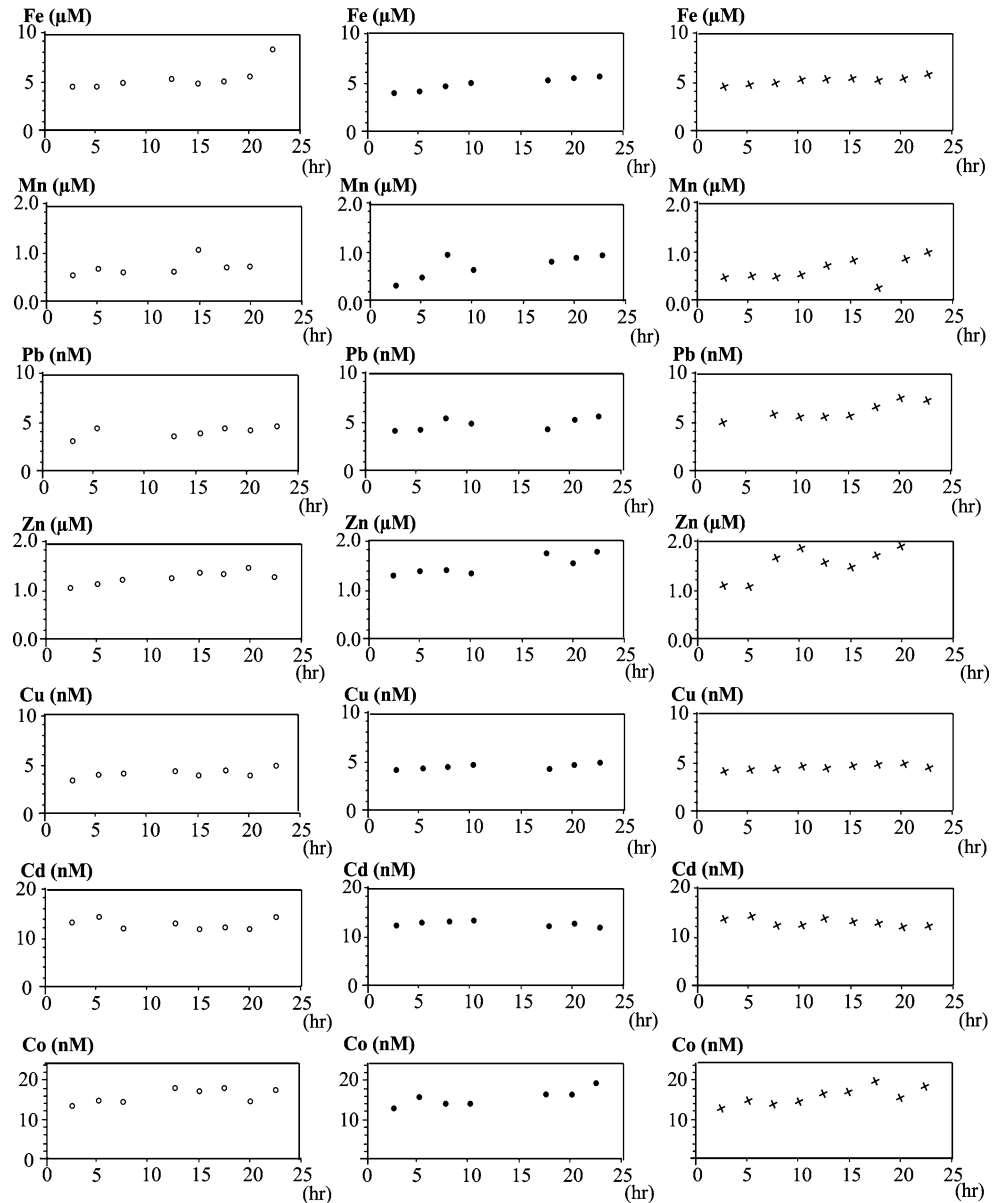
*RSD* relative standard deviation, *BDL* below detection limits

interface in March, while the maximum  $\text{Mn}^{2+}$  concentration was obtained at 1 cm below the interface, also in March (Fig. 3). Beyond 10-cm depth, the  $\text{Mn}^{2+}$  concentration decreased rapidly (below detection limits).

*Incubated water* The  $\text{Mn}^{2+}$  benthic flux was higher at the 20-m ( $160 \mu\text{mol m}^{-2} \text{day}^{-1}$ ) and at the 40-m

stations ( $150 \mu\text{mol m}^{-2} \text{day}^{-1}$ ), while it was only  $90 \mu\text{mol m}^{-2} \text{day}^{-1}$  at the 10-m station (Table 3). Seasonal variation in the  $\text{Mn}^{2+}$  concentration was not important, as confirmed by the  $\text{Mn}^{2+}$  content in the incubation water, whereas a substantial change in the concentration from 0.2 to  $1.2 \mu\text{M}$  was observed after 24 h incubation during the two seasons (Fig. 4).

**Fig. 4** Concentrations of metals measured during the 24 h of incubation experiments at stations 10 m (open circle), 20 m (filled circle) and 40 m (multi symbol) in March



• Lead

*Pore water* The release of  $Pb^{2+}$  was more abundant in August, with concentrations exceeding 100 nM, while in March the release concentration was <50 nM, as observed at all three stations. Like  $Fe^{2+}$  and  $Mn^{2+}$ , the  $Pb^{2+}$  concentration in the overlying water was very low (3–10 nM) in the pore water. The profiles of  $Pb^{2+}$  showed a strong increase in the sediment–water interface (Fig. 3). In March, the maximum concentration of  $Pb^{2+}$  was noted at 3-cm depth, while in August the peak was around 10 cm depth (Fig. 3). Below 20 cm, the dissolved lead concentration was constant (35 μM on average). *Incubated water* The  $Pb^{2+}$  concentration in the benthic chambers varied slightly from 4 to 6 nM in

August and from 3 to 5 nM in March at the 10-m station and from 5 to 7 nM offshore (Fig. 4). The benthic flux was lower near the coast ( $\sim 0.3 \mu mol m^{-2} day^{-1}$ ), whereas at the 20- and 40-m stations it was  $\sim 0.5 \mu mol m^{-2} day^{-1}$  in March, with no clear lateral variation in August (Table 3).

• Zinc

*Pore water* In August, the  $Zn^{2+}$  concentration varied from 0.1 to 2.5 μM, while in March it reached 10 μM at the 20- and 40-m stations. As with other heavy metals, the  $Zn^{2+}$  concentration in the pore water was much higher than in the water column; the concentration profiles therefore showed a more or

less rapid seasonal increase at the sediment–water interface. The release of  $Zn^{2+}$  occurred at multiple levels in the sediment, but the main peak in production occurred between 2 and 3 cm below the sediment–water interface in March and a little deeper (5–10 cm) in August (Fig. 3).

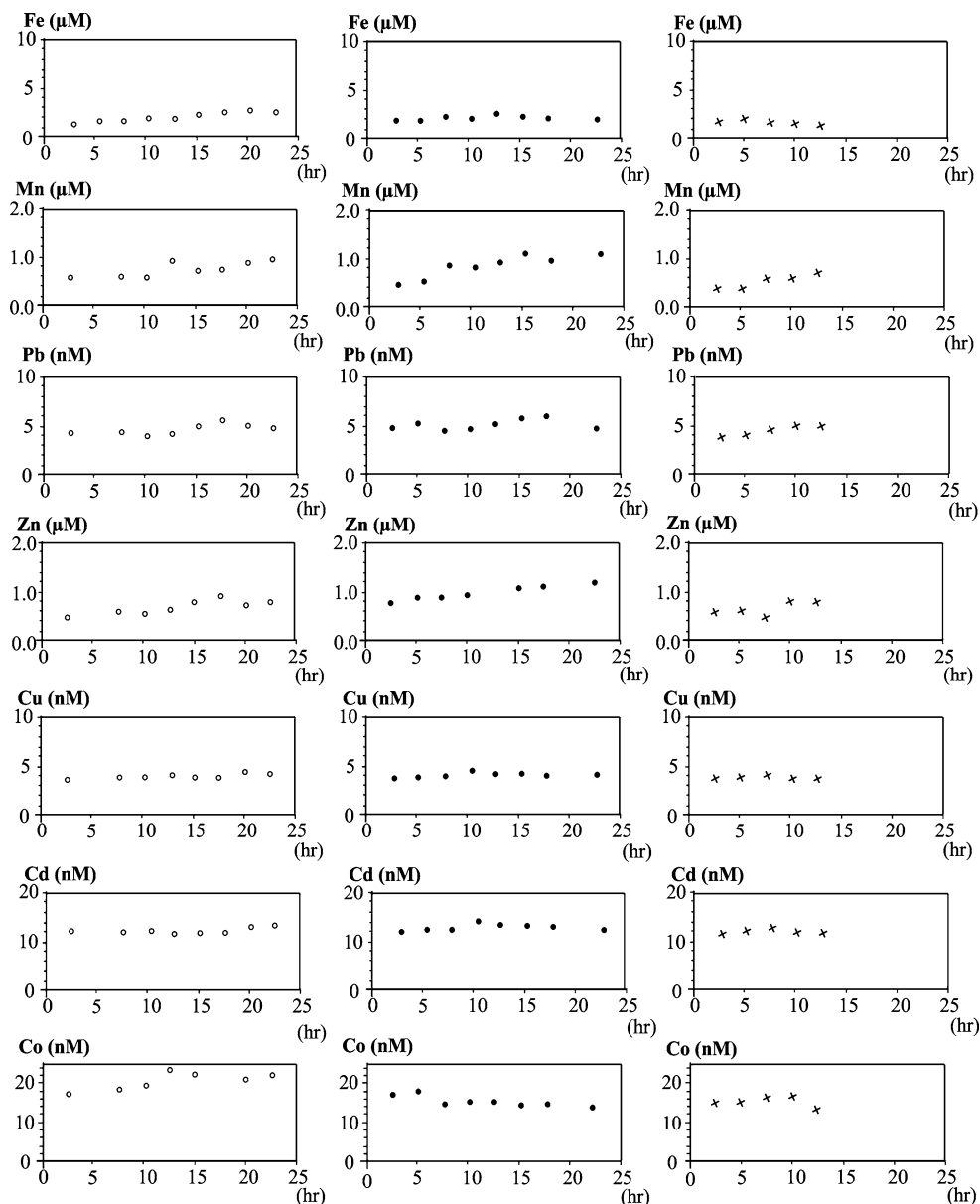
**Incubated water** As other heavy metals,  $Zn^{2+}$  content in the benthic waters gradually rose in March from 1 to 2 or 2.5  $\mu M$  within a 24-h period, according to station. This evolution was much slower in August and not always clearly established as the concentration varied between 0.5 and 1  $\mu M$  (Fig. 4), resulting in seasonal differentiation benthic fluxes. In March, the benthic flux of zinc was higher (110–270  $\mu mol m^{-2} day^{-1}$ ),

whereas in August it was 28, 77 and 134  $\mu mol m^{-2} day^{-1}$  at the 10-, 20- and 40-m stations, respectively (Table 3).

#### • Copper

**Pore water** At the bottom of the water column, the  $Cu^{2+}$  concentration did not show any significant lateral or seasonal variation (1.2–3.8 nM). However, in the pore water, the  $Cu^{2+}$  content varied greatly between the 2 months, March and August (concentration maxima were 25 and 200 nM, respectively). At the 20- and 40-m stations, the  $Cu^{2+}$  concentrations reached the same proportions in the two seasons: 150 and 80 nM at the 20- and 40-m stations,

**Fig. 5** Concentrations of metals measured during the 24 h of incubation experiments at stations 10 m (open circle), 20 m (filled circle) and 40 m (multi symbol) in August





respectively (Fig. 3), but for the maxima of  $\text{Cu}^{2+}$  there was a marked variation in depth. In fact,  $\text{Cu}^{2+}$  was localized between 2 and 5 cm below the sediment–water interface; the highest levels of  $\text{Cu}^{2+}$  were recorded in March, while the  $\text{Cu}^{2+}$  concentration in August remained a little lower in the sediment, around 12, 18 and 20 cm at the 10-, 20- and 40-m stations, slightly (Fig. 3).

**Incubated water** The  $\text{Cu}^{2+}$  concentration in the benthic chamber waters varied between 3 and 5 nM over 24 h (Fig. 5). This variation was almost the same in both seasons and at all three stations; the measured (benthic) fluxes were similar or slightly higher near the coast (0.25 and 0.38  $\mu\text{mol m}^{-2} \text{day}^{-1}$  in March and August, respectively), while further from the coast the fluxes averaged around 0.17  $\mu\text{mol m}^{-2} \text{day}^{-1}$  (Table 3).

- Cadmium

**Pore water** Cadmium was the only heavy metal whose concentration at the sediment–water interface was similar to that found in the pore water. Depending on the season, the contents of  $\text{Cd}^{2+}$  ranged from 17 to 23 nM above the sediment–water interface, whereas lower in the sediment it was 14–28 nM. In the pore water, the  $\text{Cd}^{2+}$  profiles showed a different trend between the seasons. In August, the concentration below the sediment–water interface increased, whereas in March it continued to decrease; therefore, the  $\text{Cd}^{2+}$  profile showed an opposite gradient to that observed in August as well as to that observed for other heavy metals. *In situ* measurements from the benthic chambers confirmed this trend (Fig. 3).

**Incubated water** The  $\text{Cd}^{2+}$  concentration in the benthic chamber waters did not show any significant change (Fig. 5). Thus, if the benthic fluxes are 0.38  $\mu\text{mol m}^{-2} \text{day}^{-1}$  in August, there is a reversal in their direction to  $-0.28$  to  $-0.38 \mu\text{mol m}^{-2} \text{day}^{-1}$  in March (Table 3).

- Cobalt

**Pore water** As for  $\text{Zn}^{2+}$  and  $\text{Fe}^{2+}$ , the highest levels of  $\text{Co}^{2+}$  were observed in the pore waters in March. The maximum concentration was located between 2 and 4 cm below the sediment–water interface (Fig. 3) and was higher at the 20- and 40-m stations (210 and 250 nM, respectively) than at the 10-m station (180 nM). In August, no clear gradient was observed for  $\text{Co}^{2+}$ ; in fact, at all three stations, the  $\text{Co}^{2+}$  concentration varied little across and below the sediment–water interface, as confirmed by benthic flux measurements. The concentration remained low

and constant at  $\sim 30$  nM at the 10-m station (Fig. 3). This observation confirmed the benthic chamber findings, as August is characterized by low or reversed benthic fluxes.

**Incubated water** No significant seasonal variation was observed between  $\text{Co}^{2+}$  concentrations in the benthic chamber waters, with values generally ranging between 15 and 25  $\mu\text{M}$  (Fig. 5). However, the spatial variation between benthic fluxes was important, since the fluxes measured in August were 0.29  $\mu\text{mol m}^{-2} \text{day}^{-1}$  at the 10- and 40-m station, but negative at the 20-m station ( $-38 \mu\text{mol m}^{-2} \text{day}^{-1}$ ). In March all benthic fluxes were positive, ranging from 0.96  $\mu\text{mol m}^{-2} \text{day}^{-1}$  at the 10- and 20-m stations to 1.92  $\mu\text{mol m}^{-2} \text{day}^{-1}$  at the 40-m station (Table 3).

## Discussion

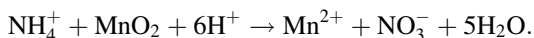
**Iron and Manganese** The benthic fluxes were most likely due to low diffusion which is considered as the main process transporting  $\text{Mn}^{2+}$  and  $\text{Fe}^{2+}$  from the sediments into estuarine water (McCaffrey et al. 1980), despite the existence of advective processes resulting from the activity of macro benthic organisms (Aller 1978). This value was lower than in Ghar El Melh Lagoon (Tunisia) in which the manganese benthic fluxes vary seasonally from 767 to 1450  $\mu\text{mol m}^{-2} \text{day}^{-1}$  (Oueslati 2011). In Thau Lagoon, France, it is about 680  $\mu\text{mol m}^{-2} \text{day}^{-1}$  (Point et al. 2007), in Baltimore Harbor, the USA, about 550  $\mu\text{mol m}^{-2} \text{day}^{-1}$  (Mason et al. 2006) while in Galveston Bay, the USA, it varies between 450 and 2300  $\mu\text{mol m}^{-2} \text{day}^{-1}$  (Warnken et al. 2001). In August, the diffusive fluxes represented a significant 8–15 % of the measured benthic flux whereas in March they were only 0.7–8 %. In all cases, these fluxes show that the sediment is a source of dissolved manganese for the water column. The diffusive fluxes showed that sediment is a source of  $\text{Fe}^{2+}$  for the water column, especially at the 10- and 20-m stations. The maximum seasonal difference was observed at the 10-m station, where the diffusive flux was 8.65  $\mu\text{mol m}^{-2} \text{day}^{-1}$  in March, but only 4  $\mu\text{mol m}^{-2} \text{day}^{-1}$  in August. The 20- and 40-m stations did not show any significant differentiation between the two seasons ( $\sim 10 \mu\text{mol m}^{-2} \text{day}^{-1}$ ). The 40-m station was characterized by the absence of a clearly established gradient below the sediment–water interface during the two seasons, as the flux was considered to be almost zero. Except for the production peaks, the concentration of dissolved iron in the pore waters was similar to those already observed in the rest of the Gulf of Tunis (9–27  $\mu\text{M}$ ) (Essoni 1998). These values were also similar to those observed in the Ghar El Melh Lagoon (20  $\mu\text{M}$ )

**Table 2** Diffusive flux of heavy metals off the Mejerda River Delta

Sites	March			August		
	10 m	20 m	40 m	10 m	20 m	40 m
Fe <sup>2+</sup> (μmol m <sup>-2</sup> day <sup>-1</sup> )	8.65	9.38	0	4.08	10.62	0
Mn <sup>2+</sup> (μmol m <sup>-2</sup> day <sup>-1</sup> )	2.57	0.93	14.63	14.22	17.9	13.04
Pb <sup>2+</sup> (nmol m <sup>-2</sup> day <sup>-1</sup> )	12.54	28.9	28.9	14.16	15.93	15.9
Zn <sup>2+</sup> (μmol m <sup>-2</sup> day <sup>-1</sup> )	2.17	3.62	3.98	0.098	0.1	0.27
Cu <sup>2+</sup> (nmol m <sup>-2</sup> day <sup>-1</sup> )	8.3	11.96	8.37	9.4	4.66	4.59
Cd <sup>2+</sup> (nmol m <sup>-2</sup> day <sup>-1</sup> )	-1.88	-1.41	-2.32	6.25	3.29	2.6
Co <sup>2+</sup> (nmol m <sup>-2</sup> day <sup>-1</sup> )	0.13	0.152	0.187	0	0	0

(Added 2002; Oueslati 2011). The diffusive fluxes of Mn<sup>2+</sup> were significantly greater in August at the 10- and 20-m stations (14.22 and 11.25 μmol m<sup>-2</sup> day<sup>-1</sup>, respectively), whereas they reached only 0.9–2.57 μmol m<sup>-2</sup> day<sup>-1</sup> in March. Offshore, the Mn<sup>2+</sup> diffusive flux did not vary much between the two seasons (~14 μmol m<sup>-2</sup> day<sup>-1</sup>) (Table 2). The concentration of Mn<sup>2+</sup> in the pore waters was similar to those observed in Ghar El Melh Lagoon (2–15 μM, Added 2002; 0–50 μM, Oueslati 2011) and higher than those found in the rest of the Gulf of Tunis (1.8–7.2 μM; Essoni 1998). Manganese production below the sediment–water interface forms a part of the overall scheme in early diagenesis of organic matter. As the gulf waters are oxygenated, manganese is found in its oxide form (MnO<sub>2</sub>) whose reduction is the main cause of increase in the dissolved manganese content in the pore water, according to the reaction:  $MO + 2x MnO_2 + (3x + y - 2z)CO_2 + (x + y - 2z)H_2O \rightarrow 2x Mn^{2+} + (3x + y - 2z)HCO_3^- + yNH_4^+ + zHPO_4$ .

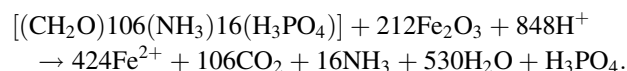
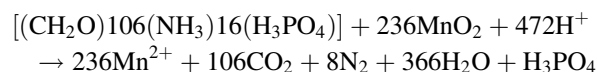
In addition to oxide reduction during the mineralization of organic matter, other chemical reactions also contribute to the origin of the Mn<sup>2+</sup> peak, with ammonium oxidation as the main source according to Hulth et al. (1999). Mn<sup>2+</sup> is produced according to the reaction:



Maximum production of Mn<sup>2+</sup> occurs at different depths, depending on the study sites and ranging from a few millimeters (as for the Mejerda Delta) to some tens of centimeters (as for Ghar El Melh Lagoon) below the sediment–water interface (Added 2002). This variation is partially due to the hydrodynamic conditions and the activity of the benthic community at the sediment–water interface. Indeed, a strong mechanical disturbance at the sediment–water interface results in the penetration of oxygen, causing the layer of manganese oxide reduction to descend even though Mn<sup>2+</sup> is not always oxidized under these aerobic conditions (Canfield et al. 1993a, b). In the case of the Mejerda Delta, all profiles show a downward shift in Mn<sup>2+</sup> production in March, without any trace of visible benthic activity at the sediment–water interface

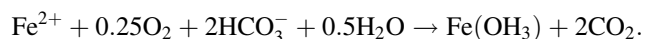
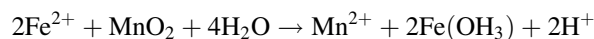
owing to a sharp rise in hydrodynamic activity in the bottom waters and greater resuspension of the sediment surface layer. In addition to the biomechanical factors responsible for sediment oxygenation, which draws Mn<sup>2+</sup> production downward to the sediment, the presence of oxygen and other chemicals, such as nitrates, may explain the heavy metal's delayed release (Sawlan and Murray 1983). However, this point was not found to be applicable at the different study sites, at least not in first few levels, despite the high nitrate concentrations observed within the reducing layer (Essoni 1998).

According to the sequences of organic matter oxidation (Froelich et al. 1979), peak Fe<sup>2+</sup> production occurs below the sediment–water interface just following Mn. This is because the degradation reaction of the organic matter involving manganese oxides liberates a greater quantity of energy ( $\Delta G = -349$  kJ/mol) as it involves iron oxides ( $\Delta G = -114$  kJ/mol) (Thauer et al. 1977). Thus, manganese oxides, followed by iron hydroxides, become the main electron acceptors in the pore water, according to the diagenetic reactions (Froelich et al. 1979; Wilson et al. 1985):



Iron and manganese are important for phytoplankton and biota development.

The release of Mn<sup>2+</sup> prior to Fe<sup>2+</sup> has been attributed to the ease with which dissolved Fe, after migrating upwards by molecular diffusion, oxidizes and precipitates as hydroxides in the presence of oxygen near the sediment–water interface (Postma 1985; Van Cappellen and Wang 1996; Martin 2005; Canavan et al. 2006), according to the reactions:



The decrease in Fe<sup>2+</sup> concentration from 15 cm is due either to the heavy metal's sequestration in the sediment or

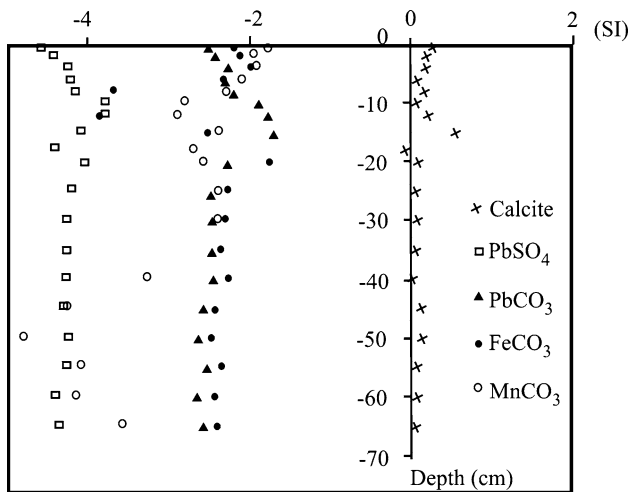
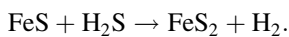
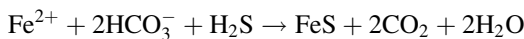


Fig. 6 Saturation indexes in 10 m sampling site

to its precipitation as carbonate (siderite  $\text{FeCO}_3$ ), even if this form is rarely observed in marine environments (Hesse 1990), or to precipitation of metal sulfides  $\text{FeS}$  and  $\text{FeS}_2$ , according to the reactions (Canavan et al. 2006):

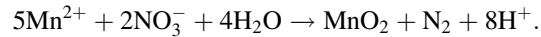


The saturation index for  $\text{FeCO}_3$  and  $\text{FeSO}_4$  obtained by the software Phreeqc was negative (Fig. 6), indicating that  $\text{Fe}^{2+}$  precipitation with carbonated minerals and/or with sulfides in the Mejerda Delta sediment is probably impossible.

The studied waters were under-saturated with these minerals, though a scanning electron microscope observation confirmed the existence of pyrite in framboidal form, more than 30 cm below the sediment–water interface (Fig. 7), and though the environment was not favorable to pyrite precipitation and according to saturation index for  $\text{FeCO}_3$  and  $\text{FeSO}_4$ . Indeed, the concentration of  $\text{H}_2\text{S}$  found there may be sufficiently high in isolated microenvironments to precipitate iron pyrite. Through these findings, it appears that the decrease in the  $\text{Fe}^{2+}$  concentration at the lowest depth of the sediment core was due to the diffusion of this metal and not to the formation of a mineral complex. As for  $\text{Mn}^{2+}$ , the reason is that the delta sediment functions on a non-stationary regime and is therefore unable to precipitate minerals.

Manganese concentrations are generally dependent on carbonate dissolution or precipitation (or co-precipitation) (Thomson et al. 1986). In the delta, the decrease in  $\text{Mn}^{2+}$  content beyond 5 cm in March and 10 cm in August may be either due to reoxidation or to precipitation with carbonates. The case of manganese reoxidation cannot be excluded considering the high concentration of nitrates

observed at these levels (Essoni 1998) and therefore the availability of oxygen, according to the reaction (Hulth et al. 1999):



The saturation index is also negative with respect to mineral carbonate species such as rhodochrosite. Unlike sulfide minerals (haurite  $\text{MnS}_2$  and alabandite  $\text{MnS}$ ), rhodochrosite cannot form in the delta sediment. Similar to  $\text{Fe}^{2+}$ , the redox conditions that characterize the delta sediment are not sufficiently reduced to permit the formation of such minerals (Helali et al. 2013). No mineral precipitation processes can explain the reduced  $\text{Mn}^{2+}$  contents in the deep layers of sediment, likely the result of the element’s diffusion. Diffusion also took place upwards, with the release of  $\text{Mn}^{2+}$  into the water column, where it is probably reoxidized by dissolved oxygen.

- **Lead** As in the pore water,  $\text{Pb}^{2+}$  concentrations at the bottom were found in the coastal areas (Morley et al. 1997), suggesting human interference from the Mejerda Delta, Ghar El Melh Lagoon (former mouth of the Mejerda River) and the Khlij Channel. When compared to benthic fluxes, diffusive fluxes represented only 0.13–3.3 % of the total at all stations because the reactions causing the release of  $\text{Pb}^{2+}$  were of greater intensity at the sediment–water interface.  $\text{Pb}^{2+}$  production in the pore water was either the result of degradation of organic matter when lead was bound to organic particles or of the reduction in iron oxides or manganese hydroxides (Widerlund et al. 2002). The  $\text{Pb}^{2+}$  content variation observed in the different pore water profiles suggests that the release of  $\text{Pb}^{2+}$  in the Mejerda River Delta is mainly via the second of these two processes. In fact, the production peak of  $\text{Pb}^{2+}$  is just below the peaks of  $\text{Mn}^{2+}$ , especially in March. The production of  $\text{Pb}^{2+}$  and  $\text{Fe}^{2+}$  shows similarity since both show a second layer of production ~20 cm below the sediment–water interface (Fig. 3). The benthic fluxes of  $\text{Pb}^{2+}$  measured in the Mejerda Delta were low compared with those of Ghar El Melh Lagoon (7–20  $\mu\text{mol m}^{-2} \text{day}^{-1}$ ) (Oueslati 2011), but were close to those of the Elbe River, Germany (0.41–0.85  $\mu\text{mol m}^{-2} \text{day}^{-1}$ ) (Petersen et al. 1995) or of Galveston Bay, the USA (0.05  $\mu\text{mol m}^{-2} \text{day}^{-1}$ ) (Warnken et al. 2001).
- **Zinc** The zinc benthic fluxes are in accordance with diffusive fluxes, with maximum diffusion in the water column varying during March at 2.17–4  $\mu\text{mol m}^{-2} \text{day}^{-1}$ . In August, they were small and difficult to estimate, ranging from 0.098  $\mu\text{mol m}^{-2} \text{day}^{-1}$  at the 10-m station and 2  $\mu\text{mol m}^{-2} \text{day}^{-1}$  at the 40-m station (Table 2). Compared to benthic fluxes, these values

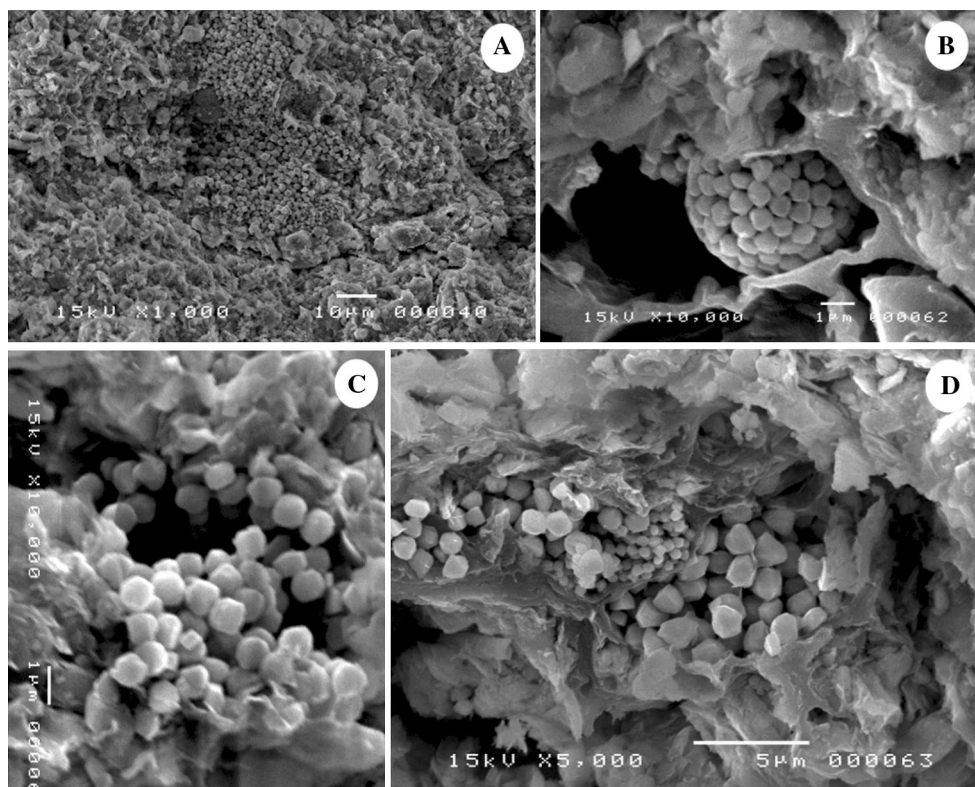


**Fig. 7** Framboidal pyrite at 30 cm (a) with dislocation forms in some microenvironment (b) and euhedral pyrite at 70 cm depth (c, d) in the 10 m sampling site

represent only 0.13–3.3 % of the total at all stations, demonstrating the importance of the magnitude of  $Zn^{2+}$  release reactions located at the sediment–water interface as opposed to those occurring at lower depths in the sediment. In other marine environments,  $Zn^{2+}$  benthic fluxes are heavy, especially in March when, for example, a flux of  $10\text{--}50\ \mu\text{mol m}^{-2}\ \text{day}^{-1}$  was measured in Ghar El Melh Lagoon (Oueslati 2011),  $15\ \mu\text{mol m}^{-2}\ \text{day}^{-1}$  in Venice Lagoon (Turetta et al. 2005), but only  $3\ \mu\text{mol m}^{-2}\ \text{day}^{-1}$  in Galveston Bay, the USA (Warnken et al. 2001). However, the highest flux value observed in this study (i.e.,  $150\ \mu\text{mol m}^{-2}\ \text{day}^{-1}$ ) was found in the Elbe River, Germany (Petersen et al. 1995). For instance, flux variability is related to (1) differences in hydrodynamics between gulfs and lagoons, (2) site geomorphology, (3) physico-chemical conditions and (4) anthropogenic activity (Schulz and Zabel 2006).

- **Copper** No significant spatial or seasonal variation in the  $Cu^{2+}$  diffusive flux was observed. Always directed toward the water column, these were in the range of  $8\text{--}11\ \text{nmol m}^{-2}\ \text{day}^{-1}$  in March and of  $4\text{--}9\ \text{nmol m}^{-2}\ \text{day}^{-1}$  in August (Table 2). Copper diffusive flux in this study could not be compared to those in other marine environments; depending on the case, the sediment is either a source of  $Cu^{2+}$  for the

water column or a well. Even if  $Cu^{2+}$  is not well correlated with  $Fe^{2+}$  and  $Mn^{2+}$  in all cores, it is normal that its evolution below the sediment–water interface recalls the values of these two metals. Indeed, copper is bound to organic matter by passive or active adsorption (Szefer 1991) when brought to the sediment surface, as in the case of the Mejerda Delta (Essoni 1998) and usually in shallow marine environments (Helland and Torgeir 2002; Morel and Hering 1993).

$Cu^{2+}$  release in the pore water is the result of organic matter degradation. Maximum degradation should coincide with maximum production of  $Cu^{2+}$  (Scholz and Neumann 2007; Tessier 2012). The  $Cu^{2+}$  produced diffuses into the water column from the deeper sediment layers where its concentration thus gradually decreases. When  $Cu^{2+}$  benthic flux is positive the values measured in the Mejerda Delta are close to those of several marine sites such as Morecambe Bay, England ( $0.25\ \mu\text{mol m}^{-2}\ \text{day}^{-1}$ ; Williams et al. 1998) and Venice Lagoon ( $0.13\ \mu\text{mol m}^{-2}\ \text{day}^{-1}$ ; Turetta et al. 2005).

- **Cadmium** The direction-reversing benthic flux observed by the incubation experiments was also confirmed by Fick's 1st law which stipulates that negative and

**Table 3** Benthic flux of heavy metals off the Mejerda River Delta

Sites ( $\mu\text{mol m}^{-2} \text{ day}^{-1}$ )	March			August		
	10 m	20 m	40 m	10 m	20 m	40 m
Fe <sup>2+</sup>	230	384	220	192	192	−38
Mn <sup>2+</sup>	86	120	170	96	160	150
Pb <sup>2+</sup>	0.3	0.48	0.5	0.5	0.23	0.42
Zn <sup>2+</sup>	190	110	270	27	77	134
Cu <sup>2+</sup>	0.25	0.17	0.17	0.384	0.115	0.23
Cd <sup>2+</sup>	−0.038	−0.282	−0.288	0.38	0.288	−0.384
Co <sup>2+</sup>	0.96	0.96	1.92	0.29	−0.38	0.29

relatively low diffusive fluxes are obtained just below the sediment–water interface (−1.4 to −2.32  $\text{nmol m}^{-2} \text{ day}^{-1}$ ), depending on the station. In August, the diffusive fluxes are in accordance with those measured in the benthic chambers (2.6–6.25  $\text{nmol m}^{-2} \text{ day}^{-1}$ ), representing only 0.67–1.6 % of total fluxes (Table 2).

The general scheme usually found in marine environments shows a peak production of Cd<sup>2+</sup> just below the sediment–water interface for cores drilled in August due to the mineralization of organic matter and release of the associated cadmium (Emerson et al. 1984; Gobeil et al. 1987; Rosenthal et al. 1995). In the Mejerda Delta cadmium appears to be associated with particulate organic matter during transport in the water column. It is then transported downwards into the sediment and upwards to diffuse into the water column. In contrast, changes in the levels of dissolved cadmium in the pore water sometimes show a pattern different from those mentioned above or observed for other metals which generally follow Fe<sup>2+</sup> and Mn<sup>2+</sup>. Indeed, some studies have shown that Cd<sup>2+</sup> in the pore water may undergo constant evolution downwards from the sediment–water interface (Gobeil et al. 1987; Rosenthal et al. 1995). Similar results were noted at all three stations during March. Cadmium benthic fluxes vary depending on study sites and seasons, but the overall values measured in the Mejerda Delta waters were similar to those observed elsewhere in the world; thus, fluxes vary from −0.6 to 5.4  $\mu\text{mol m}^{-2} \text{ day}^{-1}$  in the Ghar El Melh Lagoon (Oueslati 2011), −11 to 52  $\text{nmol m}^{-2} \text{ day}^{-1}$  in Baltimore Harbor, the USA (Mason et al. 2006) and 0.78  $\text{nmol m}^{-2} \text{ day}^{-1}$  in Thau Lagoon, France (Point et al. 2007).

- *Cobalt* Diffusive fluxes appear to be limited to March, because the concentration gradients show the existence of flux that is directed toward the water column and variable from 0.13 to 0.18  $\mu\text{mol m}^{-2} \text{ day}^{-1}$ , depending on the station. These diffusive fluxes represent only 9–16 % of benthic fluxes. In August, the concentration gradients of Co<sup>2+</sup> below the sediment–water interface

were low or non-existent and thus did not allow calculation of any fluxes according to Fick’s first law; the diffusive fluxes were thus considered void; this was confirmed by the benthic fluxes (Table 3). The benthic flux of cobalt varies considerably in marine environments. In Thau Lagoon (France), for example, the values obtained were the same as those in the Mejerda Delta (−0.35 to 4.65  $\mu\text{mol m}^{-2} \text{ day}^{-1}$ ) (Point et al. 2007). Ciceri et al. (1992) measured cobalt fluxes from 0.25 to 0.35  $\mu\text{mol m}^{-2} \text{ day}^{-1}$  in the Tyrrhenian Sea in Italy and in Ghar El Melh Lagoon and found them to be high (27–98  $\mu\text{mol m}^{-2} \text{ day}^{-1}$ ; Oueslati 2011).

### Conclusion

In the Gulf of Tunis surface sediments under oxidized conditions lead to a significant flux of Fe<sup>2+</sup> and Mn<sup>2+</sup> from the ferruginous and manganous zones of the sea floor into the lower water column. Surface sediment in the gulf can be considered as a source of dissolved iron and manganese, as illustrated by the pore water profiles and confirmed by the benthic fluxes. Surface sediment works as an iron fertilizer which may explain the frequent proliferations of phytoplankton communities with harmful algal blooms (Aissaoui et al. 2014).

The diagenetic sequence in the Mejerda River Delta for all studied stations showed the same trend. First, aerobic mineralization, a few millimeters thick and that can only be assumed below the sediment–water interface, is then followed by various anaerobic mechanisms: a reduction in manganese oxides, then a reduction in iron hydroxides to a depth of 15 cm and finally a probable sulfate reduction. All the heavy metals studied, with the exception of cobalt and cadmium, have related behaviors in pore water and then in water–sediment interface, either in the oxidation/reduction of iron oxy-hydroxides and Mn, or in the mineralization of organic matter, or both processes simultaneously. Seasonal variations cause a depth migration of the different sediment layers of production of dissolved heavy metals, probably

due to the variation of the stirring in the seabed and resuspension of surface layer sediment. This process was also responsible for the increase in the concentration of some elements, especially in March.

Except for  $\text{Cd}^{2+}$ , all heavy metals showed a significant enrichment near the sediment–water interface, though the concentrations were relatively low in the water column or at the lowest sediment depth. This variation is characteristic of pore water in marine environments and has been attributed to the degradation of organic matter freshly deposited on the bottom, as has also been reported in previous studies. In the Mejerda Delta, the concentrations of dissolved heavy metals were even higher starting in first few millimeters below the sediment–water interface. However, millimeter resolution sampling, otherwise impossible with conventional methods of pore water extraction, could be undertaken in this case. In situ measurements of benthic flux and their comparison with flux calculated using Fick's law confirmed that the degradation of freshly deposited organic matter is responsible for the release of heavy metals in the water column with few exceptions. Benthic fluxes confirm that the Mejerda Delta sediment constitutes the source of a majority of metals in the water column. Benthic and diffusive fluxes of  $\text{Fe}^{2+}$ ,  $\text{Pb}^{2+}$ ,  $\text{Zn}^{2+}$ ,  $\text{Mn}^{2+}$  and  $\text{Cu}^{2+}$  were all positive in this study. Although lateral variations appeared limited, seasonal variations were pronounced, especially for  $\text{Fe}^{2+}$ ,  $\text{Pb}^{2+}$  and  $\text{Zn}^{2+}$ ; these heavy metals appear to be more readily released in March. Cadmium and, to a lesser extent, cobalt are characterized by their reverse flux which is positive only in August. The sediment is therefore a sequestration well for cadmium and cobalt in March. The diffusive flux of heavy metals often flows in the same direction as the benthic flux, but it represents only a small fraction (0.7–30 %) of total fluxes. Compared to other similar marine environments, the benthic flux values were near the standards for all heavy metals, except for zinc which was found to be relatively high.

**Acknowledgments** This study was made possible by the Tunisian (Institut National des Sciences et Technologies de la Mer, Laboratoire des Ressources Minérales et Environnement, Faculté des Sciences de Tunis)–French (Chrono-Environnement Laboratory, Besançon, UMR CNRS 6249) cooperation project. We would like to thank all the participants for their active participation and valuable contributions.

## References

- Added A (2002) Cycles biogéochimiques des sels nutritifs, du fer, du manganèse et du soufre dans les sédiments de deux systèmes côtiers du nord de la Tunisie : lagune de Ghar El Melh et lac nord de Tunis. PhD thesis Université de Tunis El Manar
- Aissaoui A, Dhib A, Reguera B, Ben Hassine OK, Turki S, Aleya L (2014) First evidence of cell deformation occurrence during *Dinophysis* bloom along the shores of the Gulf of Tunis (SW Mediterranean Sea). *Harmful Algae* 39:191–201
- Alaoui MM, Aleya L (1995) Assessment of the eutrophication of Al Massira reservoir (Morocco) by means of a survey of the biogeochemical balance of phosphorus. *Hydrobiologia* 297:75–82
- Aller RC (1978) The effects of animal-sediment interaction on geochemical processes near the sediment-water interface. In Wiley ML (ed) *Estuarine interactions*. Academic Press, New York, pp 157–172
- Belabed B, Laffray X, Dhib A, Fertouna-Bellakhal M, Turki S, Aleya L (2013) Factors contributing to heavy metal accumulation in sediments and in the intertidal mussel *Perna perna* in the Gulf of Annaba (Algeria). *Mar Pollut Bull* 74:477–489
- Ben Salem Z, Capelli N, Grisey E, Baurand PE, Ayadi H, Aleya L (2014) First evidence of fish neurotoxicity induced by heavy metals from landfill leachates: the advantage of using the RAPD-PCR technique. *Ecotoxicol Environ Saf* 101:90–96
- Boudreau BP (1997) *Diagenetic models and their implementation*. Springer, New York
- Brahim M, Atoui A, Sammari C, Aleya L (2015) Surface sediment dynamics along with hydrodynamics along the shores of Tunis Gulf (north-eastern Mediterranean). *J Afr Earth Sci* 103:30–41
- Canavan RW, Slomp CP, Jourabchi P, Van Cappelen P, Laverman AM, Van Den Berg GA (2006) Organic matter mineralization in sediment of a coastal freshwater lake and response to salinization. *Geochim Cosmochim Acta* 90:2836–2855
- Canfield DE, Jorgensen BB, Fossing H, Glud R, Gundersen J, Ramsing NB, Thamdrup B, Hansen JW, Nielsen LP, Hall POJ (1993a) Pathways of organic carbon oxidation in three continental margin sediments. *Mar Geol* 113:27–40
- Canfield DE, Thamdrup B, Hansen JW (1993b) The anaerobic degradation of organic matter in Danish coastal sediments iron reduction, manganese reduction and sulfate reduction. *Geochim Cosmochim Acta* 57:3867–3883
- Ciceri G, Maran S, Martinotti W, Queirazza G (1992) Geochemical cycling of heavy metals in a marine coastal area—benthic flux determination from pore water profiles and in situ measurements using benthic chambers. *Hydrobiologia* 235:501–517
- Emerson S, Jahnke R, Heggie D (1984) Sediment-exchange in shallow water estuarine sediments. *J Mar Res* 42:709–730
- Essoni N (1998) Etude de la dynamique des sels nutritifs et des métaux lourds en Relation avec la sédimentologie et l'hydrodynamique dans le large du golfe de Tunis. PhD thesis. Université De Tunis II
- Froelich PN, Klinkhammer GP, Bender ML, Luedtke NA, Heath GR, Cullen D, Dauphin P, Hammond D, Hartman B, Maynard V (1979) Early oxidation of organic matter in pelagic sediments of the Eastern Equatorial Atlantic: suboxic diagenesis. *Geochim Cosmochim Acta* 43:1075–1090
- Gobeil C, Silverberg N, Sundby B, Cossa D (1987) Cadmium diagenesis in Laurentian Trough sediments. *Geochim Cosmochim Acta* 51:589–596
- Helali MA (2010) Géochimie des sédiments marins de surface dans le delta de l'Oued Mejerda. Mastère en Géologie. Université De Tunis-El Manar
- Helali MA, Oueslati W, Zaaboub N, Added A, Abdeljaouad S (2013) Geochemistry of marine sediments in the Mejerda River delta, Tunisia. *Chem Speciat Bioavailab* 25:247–257
- Helland A, Torgeir B (2002) Transport and sedimentation of Cu in a microtidal estuary, SE Norway. *Mar Pollut Bull* 44:149–155
- Hesse R (1990) Early diagenetic pore water/sediment interaction: modern offshore basins. In: McIlreath IA, Morrow DW (eds) *Diagenesis*. St. John's. Geological Association of Canada, Newfoundland, pp 277–316

- Hulth S, Aller RC, Gibert F (1999) Coupled anoxic nitrification/manganese reduction in marine sediments. *Geochim Cosmochim Acta* 63:49–66
- Martin ST (2005) Precipitation and dissolution of iron and manganese oxides. In: Grassian VH (ed) *Environmental catalysis*. CRC Press, Boca Raton
- Mason RP, Kim EH, Cornwell J, Heyes D (2006) An examination of the factors influencing the flux of mercury, methylmercury and other constituents from estuarine sediment. *Mar Chem* 102:96–110
- Mauldenhauer KM, Christoph Z, Dominik F (2008) Heavy metals as indicators for Holocene sediment provenance in a semi-arid Mediterranean catchment in northern Tunisia. *Quat Int* 189:129–134
- McCauffrey RJ, Richard J et al (1980) The relation between pore water chemistry and benthic fluxes of nutrients and manganese in Narragansett Bay, Rhode Island. *Limnol Oceanogr* 25:31–44
- Morel FMM, Hering JG (1993) *Principles and applications of aquatic chemistry*. Wiley, New York
- Morley NH, Burton JD, Tankere SPC, Martin JM (1997) Distribution and behavior of some dissolved trace metals in the western Mediterranean Sea. *Deep Res Part II Trop Stud Oceanogr* 44:675–691
- Oueslati W (2011) *Cycles biogéochimiques des métaux lourds dans les sédiments marins de la lagune de Ghar El Melh*. PhD thesis, Université Tunis El Manar
- Petersen W, Wallmann K, Li PL, Schroeder F, Knauth HD (1995) Exchange of trace elements at the sediment–water interface during early diagenesis processes. *Mar Freshw Res* 46:19–26
- Point D, Monperrus M, Tessier E, Amouroux D, Grall J, Chauvaud L, Thouzeau G, Jean F, Amice EA, Leynaert J, Clavier Donard OFX (2007) Benthic fluxes of metals (Cu, Cd, Pb, Mn, U and Hg) and organometals (MMHg, TBT, DBT and MBT) in the eutrophicated Thau Lagoon (Mediterranean Coast, France): role of the biological activity. *Estuar Coast Shelf Sci* 72:457–471
- Postma D (1985) Concentration of Mn and separation from Fe in sediments—I. Kinetics and stoichiometry of the reaction between birnessite and dissolved Fe(II) at 10 °C. *Geochim Cosmochim Acta* 49:1023–1033
- Rosenthal Y, Lam P, Boyle EA, Thomson J (1995) Authigenic cadmium enrichments in suboxic sediments: precipitation and post depositional mobility. *Earth Planet Sci Lett* 132:99–111
- Sawlan JJ, Murray JW (1983) Trace-metal remobilization in the interstitial waters of red clay and hemipelagic marine-sediments. *Earth Planet Sci Lett* 64:213–230
- Scholz F, Neumann T (2007) Trace element diagenesis in pyrite-rich sediments of the Achterwasser lagoon, SW Baltic Sea. *Mar Chem* 107:516–532
- Schulz HD, Zabel M (2006) *Marine geochemistry*. Springer, Berlin
- Szefer P (1991) Interphase and trophic relationships of metals in a southern Baltic ecosystem. *Sci Tot Environ* 101:201–215
- Tessier E (2012) *Diagnostic de la contamination sédimentaire par les métaux/metalloïdes dans la rade de Toulon et Mécanismes contrôlant leur mobilité*. PhD thesis, Chimie de l’environnement, Université du Sud Toulon Var
- Thauer RK, Jungermann K, Decker K (1977) Energy conservation in chemotrophic anaerobic bacteria. *Bact Rev* 41:100–180
- Thomson J, Higgs NC, Jarvis I, Hydes DJ, Colley S, Wilson TRS (1986) The behaviour of manganese in Atlantic carbonate sediments. *Geochim Cosmochim Acta* 50:1807–1818
- Turetta C, Capodaglio G, Cairns W, Rabar S, Cescon P (2005) Benthic fluxes of trace metals in the lagoon of Venice. *Microchem J* 79:149–158
- Van Cappellen P, Wang Y (1996) Cycling of iron and manganese in surface sediments: a general theory for the coupled transport and reaction of carbon, oxygen, nitrogen, sulfur, iron and manganese. *Am J Sci* 296:197–243
- Warnken KW, Gill GA, Griffin LL, Santchi PH (2001) Sediment–water exchange of Mn, Fe, Ni and Zn in Galveston Bay, Texas. *Mar Chem* 73:215–231
- Welch SA, Lyons WB, Kling CA (1990) A coprecipitation technique for determining trace metal concentrations in iron-rich saline solutions. *Environ Technol Lett* 11:141–144
- Widerlund A, Roos P, Gunneriusson L, Ingri J, Holmström H (2002) Early diagenesis and isotopic composition of lead in Lake Laisan, northern Sweden. *Chem Geol* 189:183–197
- Williams MR, Millward GE, Nimmo M, Fones G (1998) Fluxes of Cu, Pb and Mn to the Northeastern Irish Sea: the importance of sedimental and atmospheric inputs. *Mar Pollut Bull* 36:366–375
- Wilson TRS, Thompson J, Colley S, Hydes DJ, Higgs NC (1985) Early organic diagenesis: significance of progressive subsurface oxidation fronts in pelagic sediments. *Geochim Cosmochim Acta* 49:811–822
- Zaaboub N, Ounis A, Helali MA, Béjaoui B, Lillebø AI, Ferreira da Silva E, Aleya L (2014a) Phosphorus speciation in sediments and assessment of nutrient exchange at the water–sediment interface in a Mediterranean lagoon: implications for management and restoration. *Ecol Eng* 73:115–125
- Zaaboub N, Oueslati W, Helali MA, Abdeljaouad S, Huertas JF, Galindo AL (2014b) Trace elements in different marine sediment fractions of the Gulf of Tunis (Central Mediterranean Sea). *Chem Speciat Bioavailab* 26:1–12